sublimed at 100–110° (0.1 Torr) to give a white crystalline solid.

Dichloro(10,11-dihydro-5*H*-dibenz[*b,f*]azepin-5-yl)borane (4a). Dry benzene (50 ml) was placed in a 200-ml three-necked flask equipped with a dropping funnel, reflux condenser (acetone–Dry Ice type), gas inlet tube, and magnetic stirrer. Under stirring and cooling at *ca.* 6°, 50 mmol of BCl_3 was added. A light yellow, clear solution of 5 g (25.6 mmol) of iminodibenzyl (Aldrich, sublimed at 110° (0.1 Torr) before use) in 30 ml of dry benzene was added dropwise over 45 min, under stirring and cooling. A blue-green solid was formed. The acetone–Dry Ice condenser was replaced by ordinary reflux condenser and the reaction mixture was refluxed for 3 hr under a slow stream of dry nitrogen. The solid went in solution with HCl evolution. After the reflux period, most of the benzene was removed under normal pressure. The residue was transferred into a sublimation apparatus by syringe. After removal of the benzene, the light pink solid residue was sublimed at 100° (0.1 Torr) to give white crystals, 5.4 g (77%). *Anal.* Calcd for $Cl_2BNC_{14}H_{12}$: B, 3.92. Found: B, 3.79.

Dimethyl(10,11-dihydro-5*H*-dibenz[*b,f*]azepin-5-yl)borane (4b). Aminodichloroborane **4a**, prepared from 2 g (10 mmol) of iminodibenzyl by the preceding procedure, was dissolved in 40 ml of dry ether. To this was added under stirring a solution of 21 mmol of CH_3Li in 29 ml of ether at −80° over about 10 min. The cool bath was removed and after 3 hr of stirring the white precipitate was removed by filtration in a Schlenk apparatus. The filtered solution was yellow and clear. Most of the ether was removed by distillation at normal pressure, and the concentrated solution was transferred into a small distillation apparatus by syringe. After removing the ether in the vacuum line, the residue was distilled at 110–120° (0.1 Torr), to give a clear colorless liquid, 1.5 g (55%).

Chloromethyl(10,11-dihydro-5*H*-dibenz[*b,f*]azepin-5-yl)borane (6). To 1.00 g (3.62 mmol) of **4a** dissolved in 30 ml of dry ether was added a solution of 3.64 mmol of CH_3Li dissolved in 6.5 ml of ether. The solution was cooled at −20° and stirred during the addition, which required 5 min. After 1 hr of stirring at −20°, the white precipitate was removed by filtration in a Schlenk apparatus. Most of the ether was distilled under normal pressure and the residue was transferred in a small distillation apparatus attached to the vacuum line by syringe, while nitrogen gas was blowing through the apparatus. Ether was then removed completely. The residue, a very viscous, colorless liquid, was distilled into an nmr tube at 120–150° (0.1 Torr). The yield was about 500 mg (54%).

Acknowledgment. The authors wish to acknowledge financial support for this work by the National Science Foundation, through Grant GP-7101.

Registry No. **1a**, 1139-65-7; **1b**, 950-80-1; **2a**, 52760-79-9; **2b**, 52760-80-2; **3a**, 52760-81-3; **3b**, 52760-82-4; **4a**, 52760-83-5; **4b**, 52760-84-6; **6**, 52760-85-7; acridane, 92-81-9; 4,5-dimethylacridane, 52760-86-8; iminodibenzyl, 494-19-9; BCl_3, 10294-34-5; ^{11}B, 14798-13-1.

Contribution from the Chemistry Department,
University of Southern California, Los Angeles, California 90007

Microwave Spectrum, Structure, and Dipole Moment of Aminodiborane

KAR-KUEN LAU, ANTON B. BURG, and ROBERT A. BEAUDET*

Received April 12, 1974 AIC40237I

The microwave spectra of ten isotopic species of $H_2NB_2H_5$ have been assigned. The following substitution values for the structural parameters were determined: r(B–B) = 1.916 ± 0.002 Å, r(B–N) = 1.558 ± 0.001 Å, r(B–H_{br}) = 1.355 ± 0.005 Å, r(B–H_t) = 1.193 ± 0.001 Å, ∠BNB = 75.9 ± 0.1°, ∠$BH_{br}B$ = 90.0 ± 0.6°, ∠H_tBH_t = 121.0 ± 0.3°, ϵ = 16.8 ± 0.1°. From the center of mass equations, the amino hydrogen parameters were calculated to be r(N–H) = 1.005 ± 0.006 Å and ∠HNH = 111.0 ± 1.2°. The dipole moment was measured to be 2.67 ± 0.03 D. Also the ^{14}N nuclear quadrupole coupling constants were found to be χ_{aa} = −2.71 ± 0.03 MHz, χ_{bb} = 0.84 ± 0.05 MHz, and χ_{cc} = 1.87 ± 0.08 MHz.

Introduction

For the last few years, the molecular structures and properties of small carboranes have been the subjects of investigation in this laboratory. In the course of these studies, it became apparent that the structure of aminodiborane (ADB), a small, common cyclic diborane derivative, was never properly determined, probably because ADB is unstable and decomposes gradually at ambient temperatures. In an early electron diffraction study on ADB, the difficulties in discriminating closely spaced, nonequivalent internuclear distances led to large uncertainties in the structure.[1] Also, the present log sector method of electron diffraction was not used, and the experimental results might include effects from some decomposition products. An attempt was made in this laboratory to determine the structure of the more stable *N,N*-dimethyl derivative of this compound.[2] However, because the heavy methyl groups shifted the center of mass close to the nitrogen atom, an accurate structure determination was not possible. Accordingly, we have studied the rotational spectrum of the parent ADB.

The microwave spectra of ten isotopic species of ADB have been obtained. From these data, an accurate molecular structure was determined. Since the spectra of both singly isotopically substituted and doubly isotopically substituted species were assigned, all ambiguities in the signs of the center of mass coordinates were resolved and the internal consistency afforded a check on the precision of the results. The final structure is given in Figure 1. We refer to the terminal and bridge hydrogen atoms as H_t and H_{br}, respectively. The nuclear quadrupole coupling constants of the nitrogen were determined. Also, the dipole moment was measured by determining the Stark effect for selected transitions.

Experimental Section

Various isotopic species of ADB were made by the original procedure,[3] slightly modified to employ smaller quantities of the available rare isotopic reagents. The "diammoniate of diborane," $(NH_3)_2BH_2^+BH_4^-$, was formed in a small U tube in a high-vacuum system. It was treated repeatedly with diborane in excess, with brief exposure to temperatures as high as 90° and immediate removal of hydrogen and other volatiles, from which small yields of the desired ADB were isolated and accumulated. Finally, the accumulated product was purified very carefully by high-vacuum fractional condensation. The ^{15}N species were made from 99.9% enriched $^{15}NH_3$, obtained as a gas from Stohler Chemical Co., Azusa, Calif.

Due to the rather large dipole moment of ADB, lines were ex-

(1) K. Hedberg and A. J. Stosick, *J. Amer. Chem. Soc.*, 74, 954 (1952).

(2) E. A. Cohen and R. A. Beaudet, *Inorg. Chem.*, 12, 1570 (1973).

(3) H. I. Schlesinger, D. M. Ritter, and A. B. Burg, *J. Amer. Chem. Soc.*, 60, 2297 (1938).

Table I. Rotational Transitions for the Nitrogen and Boron Isotopes of $NH_2B_2H_5$ (MHz)[a]

	Isotope									
	Normal		$^{14}N^{10}B^{11}B$		$^{14}N^{10}B^{10}B$		$^{15}N^{11}B^{11}B$		$^{15}N^{10}B^{11}B$	
Transitions	ν_{obsd}	Δ	ν_{obsd}	Δ	ν_{obsd}	Δ	ν_{obsd}	Δ	ν_{obsd}	Δ
$0_{00} \rightarrow 1_{11}$[b]	29,547.68	0.00	29,951.30	0.00	30,336.02	0.00	28,991.04	0.00	29,399.16	0.00
$2_{12} \rightarrow 2_{21}$	28,051.1	0.9	27,849.3	1.1	27,567.8	0.9	27,097.2	0.7	26,922.6	0.9
$3_{03} \rightarrow 3_{12}$	25,385.4	0.8	26,033.1	0.9	26,749.5	0.5	25,790.8	0.6	26,450.9	0.3
$3_{13} \rightarrow 3_{22}$	35,139.0	1.2	35,218.4	1.2	35,258.0	1.3	34,452.8	1.0	34,564.8	0.8
$3_{22} \rightarrow 3_{31}$[b]	37,320.41	0.00	36,701.91	0.00	35,924.19	0.00	35,519.13	0.00	34,948.74	0.00
$3_{21} \rightarrow 3_{30}$[b]	30,715.79	0.00	29,664.21	0.00	28,384.67	0.00	28,402.72	0.00	27,392.94	0.00
$4_{04} \rightarrow 4_{13}$	38,766.6	0.2	39,742.1	0.2			39,351.6	0.0		
$4_{13} \rightarrow 4_{22}$	22,865.56	0.04	23,236.28	−0.02	23,690.12	−0.28	22,925.35	−0.11	23,379.78	−0.08
$4_{23} \rightarrow 4_{32}$							39,587.42	−0.20	39,315.53	−0.20
$4_{22} \rightarrow 4_{31}$[b]	27,042.13	0.34	26,085.22	0.37	24,974.70	−0.46	24,975.72	0.35	24,119.94	0.27
$5_{14} \rightarrow 5_{23}$	33,005.01	−1.84	34,092.59	−2.08	35,345.10	−2.56	33,919.39	−2.17	35,058.60	−2.28
$5_{23} \rightarrow 5_{32}$	26,050.54	−0.01	25,623.86	−0.07	25,198.46	−0.24	24,838.42	−0.25	24,581.13	−0.29
$5_{32} \rightarrow 5_{41}$					38,069.8	0.1	38,264.41	−0.27	36,629.70	−0.22
$6_{24} \rightarrow 6_{33}$	30,075.60	−2.40	30,571.24	−2.68	31,262.25	−3.40	30,195.29	−3.02	30,902.54	−3.30
$6_{33} \rightarrow 6_{42}$	36,639.4	0.6	35,069.4	0.5	33,298.6	0.8	33,439.27	0.49	32,077.85	0.37
$7_{25} \rightarrow 7_{34}$	39,942.59	−8.05								
$7_{34} \rightarrow 7_{43}$	34,108.10	−0.46	33,329.78	−0.97	32,620.35	−1.65	32,220.49	−1.43	31,794.73	−2.03
$8_{35} \rightarrow 8_{44}$	37,014.63	−6.39	37,565.82	−7.70	38,480.42	−9.58	37,117.68	−8.35	38,089.14	−9.66
$8_{44} \rightarrow 8_{53}$									39,769.77	1.38

[a] Lines reported to 0.01 MHz have been measured to better than ±0.05 MHz. Lines reported to 0.1 MHz have been measured to better than ±0.2 MHz. Δ is defined as $\nu_{calcd} - \nu_{obsd}$. [b] Frequency of the hypothetical unsplit line from analysis of the ^{14}N nuclear quadrupole hyperfine structure; the other measurements are of the mean frequency of the unresolved or partially resolved lines.

Table II. Rotational Transitions for the Monodeuterated Species of $^{14}NH_2B_2H_5$ (MHz)[a]

	$^{11}B^{11}BD_t$		$^{11}B^{10}BD_t$		$^{10}B^{11}BD_t$		$^{11}BD_b{}^{11}B$		$^{11}BD^{10}B$	
Transitions	ν_{obsd}	Δ	ν_{obsd}	Δ	ν_{obsd}	Δ	ν_{obsd}	Δ	ν_{obsd}	Δ
$0_{00} \rightarrow 1_{11}$[b]	28,120.60	0.00	28,413.85	0.00	28,541.86	0.00	27,834.55	0.00	28,176.0	0.00
$1_{11} \rightarrow 2_{02}$	38,393.8	−0.8	39,524.3	−0.9	39,498.2	−0.5				
$2_{12} \rightarrow 2_{21}$	26,943.3	0.8	26,658.2	0.9	26,875.1	0.4	25,074.8	0.8	24,824.0	0.8
$3_{03} \rightarrow 3_{12}$	21,753.0	0.8	22,271.5	0.8	22,153.8	1.9	26,756.9	0.7	27,500.9	0.8
$3_{13} \rightarrow 3_{22}$	32,705.4	1.1	32,656.5	1.1	32,804.3	1.8	33,066.5	1.0	33,162.9	0.7
$3_{22} \rightarrow 3_{31}$[b]	36,992.93	0.00	36,268.03	0.00	36,696.95	0.00	31,690.07	0.00	30,968.47	0.00
$3_{21} \rightarrow 3_{30}$[b]	32,132.77	0.00	31,043.77	0.00	31,597.6	0.0	23,391.93	0.00	22,146.23	0.00
$4_{04} \rightarrow 4_{13}$	33,046.4	0.1	33,923.5	0.2	33,713.0	1.9				
$4_{13} \rightarrow 4_{22}$	20,581.52	0.41	20,706.08	0.22	20,732.94	0.79	23,528.12	−0.33	24,233.14	−0.41
$4_{23} \rightarrow 4_{32}$	39,656.5	0.1	39,151.4	0.1	39,503.7	0.5	36,649.4	−0.2	36,337.3	−0.2
$4_{22} \rightarrow 4_{31}$	28,651.9	0.1	27,544.3	−1.7	28,088.9	−0.1	20,890.3	0.2	20,042.4	0.2
$4_{31} \rightarrow 4_{40}$							35,711.4	−1.2	33,819.6	2.1
$5_{14} \rightarrow 5_{23}$	27,755.36	−1.00	28,538.68	−1.05	28,335.32	0.27	36,203.71	−2.50	37,546.56	−2.39
$5_{23} \rightarrow 5_{32}$	26,401.32	0.35	25,630.56	0.42	26,026.90	0.3	23,081.78	−0.72	23,168.94	−0.92
$5_{32} \rightarrow 5_{41}$							30,622.8	0.6	28,710.8	0.3
$6_{15} \rightarrow 6_{24}$	38,832.88	−3.53			39,834.28	−0.29				
$6_{24} \rightarrow 6_{33}$	27,540.83	−0.74	27,484.7	−1.0	27,599.90	−0.41	31,642.67	−4.25	32,943.55	−4.71
$6_{33} \rightarrow 6_{42}$	39,872.41	0.33	38,044.90	0.66	38,912.5	−0.1	27,484.7	0.1	26,379.76	−0.24
$7_{25} \rightarrow 7_{34}$	33,307.26	−4.31	34,244.84	−4.96	33,991.37	−3.21				
$7_{34} \rightarrow 7_{43}$	35,771.33	1.17	34,333.43	0.95	35,018.77	0.49	30,031.57	−3.76	30,437.64	−4.74
$7_{43} \rightarrow 7_{52}$							37,276.28	1.63	34,673.21	1.49
$8_{35} \rightarrow 8_{44}$	34,843.90	−1.37	34,371.79	−2.21	34,663.13	−1.57	39,664.42	−12.84		
$8_{44} \rightarrow 8_{53}$							33,776.99	−0.27	32,519.53	−1.68

[a] Lines reported to 0.01 MHz have been measured to better than ±0.05 MHz. Lines reported to 0.1 MHz have been measured to better than ±0.2 MHz. Δ is defined as $\nu_{calcd} - \nu_{obsd}$. [b] Frequency of the hypothetical unsplit line from analysis of the ^{14}N nuclear quadrupole hyperfine structure; the other measurements are of the mean frequency of the unresolved or partially resolved lines.

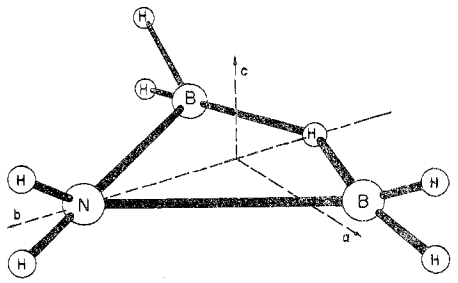

Figure 1. Principal axis orientation in aminodiborane.

pected to be intense. Hence the sample was used without further purification to remove higher boranes and ammonia gas.

ADB is extremely sensitive to moisture. Even in the absence of moisture, it decomposes slowly at room temperature. Therefore, the Stark cell was cooled with Dry Ice in order to reduce thermal decomposition and to lower the water vapor pressure arising from desorption from the cell surfaces. This Dry Ice cooling proved quite satisfactory. Even though no effort was made to cool the sample inlet tube (flexible steel tubing 1 m length), a fresh sample was required only after an interval of 3 hr.

The rotational spectrum in the 18.5–40 GHz region was observed with a Hewlett-Packard 8400C MRR spectrometer. The sample pressure used in the final measurements varied from below 5 to 10 μ depending on the abundance of the isotopic species. Trace amounts of pentaborane and ammonia gas were observed in addition to the spectrum of ADB. No evidence of the perdeuterio species of ADB was found.

Spectrum Assignment

The spectrum is that of an asymmetric top with b-type selection rules. The low-J transitions were intense and readily identified from their characteristic Stark effects. As de-

Table III. Rotational Constants and Moments of Inertia of the Isotopic Species of $H_2NB_2H_5$[a]

Isotopic species	A, MHz	B, MHz	C, MHz	I_a, amu Å^2	I_b, amu Å^2	I_c, amu Å^2
$^{14}N^{11}B^{11}B$	19,448.87	14,228.18	10,098.81	25.9928	35.5302	50.0584
$^{14}N^{11}B^{10}B$	19,617.02	14,604.47	10,334.28	25.7700	34.6148	48.9178
$^{14}N^{10}B^{10}B$	19,762.49	15,001.03	10,573.53	25.5803	33.6997	47.8109
$^{15}N^{11}B^{11}B$	19,011.60	14,228.69	9,979.44	26.5906	35.5289	50.6572
$^{15}N^{11}B^{10}B$	19,186.54	14,603.39	10,212.62	26.3482	34.6173	49.5006
$^{11}B^{11}BD_t$	18,550.72	12,988.15	9,569.89	27.2512	38.9224	52.8251
$^{11}B^{10}BD_t$	18,649.80	13,303.78	9,764.05	27.1065	37.9990	51.7747
$^{10}B^{11}BD_t$	18,750.05	13,297.33	9,791.81	26.9615	38.0174	51.6279
$^{11}B^{11}BD_b$	18,096.28	14,261.12	9,738.27	27.9356	35.4481	51.9117
$^{11}B^{10}BD_b$	18,225.19	14,636.43	9,950.81	27.7380	34.5392	50.8030

[a] Estimated errors in the rotational constants are ±0.05 MHz or better. The conversion factor to convert MHz to amu Å^2 was 5.05531×10^5 MHz amu Å^2. These constants were calculated from the $0_{00} \rightarrow 1_{11}$, $3_{22} \rightarrow 3_{31}$, and $3_{21} \rightarrow 3_{30}$ lines in each species.

Table IV. Quadrupole Splittings in ^{14}N Isotopic Species of $NH_2B_2H_5$ (MHz)[a]

		ν_{obsd}							
Transitions	$F \rightarrow F'$	$^{11}B^{11}B$	$^{11}B^{10}B$	$^{10}B^{10}B$	$^{11}B^{11}BD_t$	$^{11}B^{10}BD_t$	$^{10}B^{11}BD_t$	$^{11}B^{11}BD_b$	$^{11}B^{10}BD_b$
$0_{00} \rightarrow 1_{11}$	1 → 2	29,547.64	29,951.26	30,335.98					
	1 → 1	29,547.90	29,951.52	30,336.26					
$\Delta\nu_{obsd}$		−0.26	−0.26	−0.28					
$\Delta\nu_{calcd}$		−0.25	−0.26	−0.25					
$3_{22} \rightarrow 3_{31}$	4 → 4	37,320.14	36,701.64	35,923.92	36,992.66	36,267.76	36,696.68	31,689.80	30,968.20
	3 → 3	37,321.28	36,702.78	35,925.06	36,993.82	36,268.88	36,697.80	31,690.90	30,969.35
$\Delta\nu_{obsd}$		−1.14	−1.14	−1.14	−1.16	−1.12	−1.12	−1.10	−1.15
$\Delta\nu_{calcd}$		−1.13	−1.14	−1.13	−1.14	−1.13	−1.14	−1.12	−1.11
$3_{21} \rightarrow 3_{30}$	4 → 4	30,715.52	29,663.94	28,384.40	32,132.50	31,043.50	31,597.3	23,391.66	22,145.96
	3 → 3	30,716.62	29,665.10	28,385.50	32,133.58	31,044.62	31,598.4	23,392.74	22,147.08
$\Delta\nu_{obsd}$		−1.10	−1.16	−1.10	−1.08	−1.12	−1.1	−1.08	−1.12
$\Delta\nu_{calcd}$		−1.10	−1.10	−1.11	−1.14	−1.13	−1.1	−1.10	−1.10
$4_{22} \rightarrow 4_{31}$	5 → 5	27,041.97	26,085.06						
	4 → 4	27,042.50	26,085.58						
$\Delta\nu_{obsd}$		−0.53	−0.52						
$\Delta\nu_{calcd}$		−0.61	−0.58						

[a] Components of ^{14}N quadrupole coupling tensor in principal axes of the most abundant species are $\chi_{aa} = -2.71 \pm 0.03$ MHz, $\chi_{bb} = 0.84 \pm 0.05$ MHz, and $\chi_{cc} = 1.87 \pm 0.08$ MHz.

scribed later in the ^{14}N nuclear quadrupole coupling section, we were able to observe the ^{14}N quadrupole hyperfine structure in several low-J lines. Only two out of three hyperfine components were resolved. The hyperfine structure was assigned from the relative intensity of the two components and a simulation of the hyperfine splittings. The frequencies of the assigned transitions are cited in Tables I and II. The rotational constants and moments of inertia for all assigned isotopic species are given in Table III. Table IV gives the ^{14}N hyperfine structures.

Dipole Moment

Stark effect measurements were made on the $|M| = 1, 2, 3, 4$ lobes of the $4_{22} \leftarrow 4_{13}$ transition. The observed Stark coefficients are given in Table V. The cell spacing was determined using the $2 \leftarrow 1$ transition of OCS.[4] The dipole moment was determined to be 2.67 ± 0.03 D. Comparing with *N,N*-dimethylaminodiborane (DMADB) the value increases by 0.1 D when the two methyl groups are substituted on the bridge nitrogen atom.

^{14}N Nuclear Quadrupole Coupling

The low-J lines of ADB are broadened by the interaction of the boron and nitrogen quadrupole coupling to the molecular rotation. Among those lines which had resolvable fine structure, the $3_{31} \leftarrow 3_{22}$ and $3_{30} \leftarrow 3_{21}$ lines in all eight ^{14}N isotopic species of ADB closely resembled a well-resolved asymmetry doublet. The fine structure of these proved to be identical for the ^{10}B and ^{11}B isotopes even though the quadrupole moment of ^{10}B is twice that of ^{11}B and the spins are different. Also these same transitions in the ^{15}N isotopic species of ADB were symmetric and narrow. Therefore we could discern that the lines which have significant ^{14}N and negligible boron quadrupolar effects from those which have complicated quadrupole effects. From the hyperfine structure given in Table IV, the components of the ^{14}N quadrupole coupling tensor in the principal axes of the normal species were calculated to be $\chi_{aa} = -2.71 \pm 0.03$ MHz, $\chi_{bb} = 0.84 \pm 0.05$ MHz, and $\chi_{cc} = 1.87 \pm 0.08$ MHz.

Table V. Stark Effect in $NH_2B_2H_5$

Transition	$10^5\Delta\nu/E^2$, MHz (cm/V)^2	μ_b, D
$4_{13} \rightarrow 4_{22}, M = 1$	0.113	2.65 ± 0.03
$4_{13} \rightarrow 4_{22}, M = 2$	0.586	2.68 ± 0.03
$4_{13} \rightarrow 4_{22}, M = 3$	1.369	2.68 ± 0.03
$4_{13} \rightarrow 4_{22}, M = 4$	2.472	2.68 ± 0.03
		Av 2.67 ± 0.03

Molecular Structure

Since all monosubstituted ^{10}B, ^{15}N, D_t, and D_{br} species have been studied, the coordinates of every atom except those of the two amino hydrogen atoms were determined by the Kraitchman method.[5] Rotational constants used in obtaining the coordinates have been determined from the same transitions for each isotopic species. In this way, vibration–rotation effects such as those of centrifugal distortion will tend to cancel. Coordinates of atoms in the principal axis frames of the different reference species are given in Table VI.

From the Kraitchman equations, an r_s structure is determined. The r_s values differ from the true equilibrium values, r_e, due to hidden vibrational effects. It is important to esti-

(4) J. S. Muenter, *J. Chem. Phys.*, **48**, 4544 (1968).

(5) J. Kraitchman, *Amer. J. Phys.*, **21**, 17 (1953).

Table VI. Coordinates of Atoms in Principal Axis Systems of Reference Species[a]

	Coordinate	$^{14}N^{11}B^{11}B$	$^{14}N^{11}B^{10}B$	$^{14}N^{10}B^{10}B$	$^{15}N^{11}B^{11}B$	$^{15}N^{11}B^{10}B$	$^{14}N^{11}B$-$^{11}BD_t$	$^{14}N^{11}B$-$^{10}BD_t$	$^{14}N^{10}B$-$^{11}BD_t$	$^{14}N^{11}B$-$^{11}BD_b$	$^{14}N^{11}B$-$^{10}BD_b$
B_1	*a*	0.9588	0.9574	0.9588	0.9589		0.9543	0.9517		0.9571	
	b	−0.4454	−0.4092	−0.4670	−0.4632		−0.5129	−0.5685		−0.4138	
	c	0.000	0.000	0.000	0.000		0.000	0.000		0.000	
B_2	*a*	−0.9588	−0.9579	−0.9588	−0.9589	−0.9537	−0.9526		−0.9626	−0.9571	−0.9523
	b	−0.4454	−0.5038	−0.4670	−0.4632	−0.5271	−0.3505		−0.3887	−0.4138	−0.4809
	c	0.000	0.000	0.000	0.000	0.000	−0.0912		−0.0977	0.000	0.000
N_3	*a*	0.000	−0.0609[b]		0.000	−0.0610[b]					
	b	0.7838	0.7712		0.7661	0.7529					
	c	0.000	0.000		0.000	0.000					
H_4	*a*	0.000	0.0467[b]							0.000	0.000
	b	−1.3975	−1.4070							−1.3800	−1.3887
	c	0.0	0.0							0.0556	0.0559
H_5	*a*	1.5212	1.5275								
	b	−0.6149	−0.5504								
	c	1.0383	1.0385								
H_6	*a*	1.5212	1.5275								
	b	−0.6149	−0.5504								
	c	−1.0383	−1.0385								
H_7	*a*	−1.5212	−1.5114				−1.5915	−1.5920	−1.6002		
	b	−0.6149	−0.7009				−0.5090	−0.4485	−0.5698		
	c	1.0383	1.0382				0.8989	0.8987	0.8890		
H_8	*a*	−1.5212	−1.5114								
	b	−0.6149	−0.7009								
	c	−1.0383	−1.0382								

[a] These coordinates were determined by Kraitchman's monosubstituted method. [b] Determined by symmetry.

Table VII. Coordinates of Atoms in the Principal Axis System of the Normal $NH_2B_2H_5$

	Coordinate	$^{14}N^{11}B$-^{11}B	$^{14}N^{11}B$-^{10}B	$^{14}N^{10}B$-^{10}B	$^{15}N^{11}B$-^{11}B	$^{15}N^{11}B$-^{10}B	$^{14}N^{11}B$-$^{11}BD_t$	$^{14}N^{11}B$-$^{10}BD_t$	$^{14}N^{10}B$-$^{11}BD_t$	$^{14}N^{11}B$-$^{11}BD_b$	$^{14}N^{11}B$-$^{10}BD_b$	Av ± std
B_1	*a*	0.9588	0.9585	0.9588	0.9589		0.9581	0.9582		0.9571		0.9582 ± 0.0008
	b	−0.4454	−0.4458	−0.4454	−0.4455		−0.4456	−0.4454		−0.4457		−0.4454 ± 0.0003
	c	0.000	0.000	0.000	0.000		0.000	0.000		0.000		0.000
B_2	*a*	−0.9588	−0.9591	−0.9588	−0.9589	−0.9592	−0.9577		−0.9577	−0.9571	−0.9570	−0.9582 ± 0.0008
	b	−0.4454	−0.4448	−0.4454	−0.4455	−0.4449	−0.4457		−0.4457	−0.4457	−0.4457	−0.4454 ± 0.0003
	c	0.000	0.000	0.000	0.000	0.000	0.00		0.00	0.000	0.000	0.000
N_3	*a*	0.000	0.000		0.000	0.000						0.000
	b	0.7838	0.7838		0.7838	0.7835						0.7837 ± 0.0002
	c	0.000	0.000		0.000	0.000						0.000
H_4	*a*	0.000	0.000							0.000	0.000	0.000
	b	−1.3975	−1.3970							−1.4119	−1.4085	−1.4037 ± 0.0065
	c	0.0	0.0							0.0	0.0	0.0
H_5	*a*	1.5212	1.5208									1.5209 ± 0.0006
	b	−0.6149	−0.6153									−0.6150 ± 0.0005
	c	1.0383	1.0385									1.0385 ± 0.0004
H_6	*a*	1.5212	1.5208									1.5209 ± 0.0006
	b	−0.6149	−0.6153									−0.6150 ± 0.0005
	c	−1.0393	−1.0385									−1.0385 ± 0.0004
H_7	*a*	−1.5212	−1.5217									−1.5209 ± 0.0006
	b	−0.6149	−0.6141									−0.6150 ± 0.0005
	c	1.0383	1.0382									1.0385 ± 0.0004
H_8	*a*	−1.5212	−1.5217									1.5209 ± 0.0006
	b	−0.6149	−0.6141				−1.5202	−1.5199	−1.5205			−0.6150 ± 0.0005
	c	−1.0383	−1.0382				−0.6156	−0.6159	−0.6153			−1.0385 ± 0.0004
							1.0392	1.0394	1.0392			
H_9[a]	*a*											0.000
	b											1.3528 ± 0.0089
	c											0.8282 ± 0.0010
H_{10}[a]	*a*											0.000
	b											1.3528 ± 0.0089
	c											−0.8282 ± 0.0010

[a] The *b* coordinate was determined by $\Sigma_i m_i b_i = 0$. The *c* coordinate was determined by the relation $(I_a + I_b - I_c)/2 = \Sigma_i m_i c_i^2$.

mate the accuracy of a structure determined by rotational spectroscopy. To find the r_e structure would require a complete knowledge of all the vibrational states and their values. For a large molecule, this is practically impossible: only the r_s structures can be obtained. Also, it is necessary to estimate the accuracy of the r_s structure. Usually, the accuracy of the coordinates is estimated from the assumed errors in the moments of inertia. When sufficient data are available, a more realistic appraisal can be made from the statistical spread in the determined coordinates for each atom.

In order to do this, we have calculated the atomic coordinates obtained from each reference species in the principal axis system of the most abundant isotopic species. Here we have the monosubstituted coordinates of every atom except those of the two amino hydrogen atoms. By symmetry, only two independent coordinates are needed to define these

Table VIII. Structure of $NH_2B_2H_5$

	$NH_2B_2H_5$			
	This work[a]	Ref 1	$(CH_3)_2NB_2H_5$[c]	B_2H_6[d]
B–B, Å	1.916 ± 0.002	1.93 ± 0.10	1.916 ± 0.004	1.762_8 ± 0.0026
B–N, Å	1.558 ± 0.001	1.564 ± 0.026	1.544 ± 0.0010	
$B–H_{br}$, Å	1.355 ± 0.005		1.365 ± 0.006	1.320_4 ± 0.0010
$B–H_t$, Å	1.193 ± 0.001	1.15 ± 0.09	$1.191 \begin{smallmatrix}+0.010\\-0.003\end{smallmatrix}$	1.200_5 ± 0.0036
N–H, R	1.005 ± 0.006			
BNB, deg	75.9 ± 0.1	76.2 ± 2.8	76.8 ± 1	
$BH_{br}B$, deg	90.0 ± 0.6		89.1 ± 0.9	83.8 ± 0.2
H_tBH_t, deg	121.0 ± 0.3		119.6 ± 0.5	121.0 ± 0.6
HNH, deg	111.0 ± 1.2			
ϵ,[b] deg	16.8 ± 0.1	15 ± 20	16.7 ± 1	

[a] The quoted errors are from the standard deviations in Table VII. [b] ϵ is the angle made by the BH_2 plane and the plane perpendicular to the C_{2v} symmetry axis. [c] Reference 2. [d] W. J. Lafferty, *J. Mol. Spectrosc.*, **33**, 345 (1970).

two amino hydrogen atoms. They are obtained by the center of mass equation

$$\sum_i m_i b_i = 0$$

and the relation

$$(I_a + I_b - I_c)/2 = \sum_i m_i c_i^2$$

The coordinates in Table VI are then transformed into the principal axes of the most abundant species by appropriate rotation and translation of the axes. Since these changes are small, the corrections are not highly sensitive to the molecular structure. The final results after the transformation are presented in Table VII. The average and standard deviations were calculated by assuming C_{2v} symmetry which was indeed confirmed by the observed relative intensity among different isotopic species. Again the coordinates of the two amino hydrogen atoms were determined as stated above. The standard deviations calculated in this manner are of the same order of magnitude as the standard deviations from uncertainties in measurements.

Discussion

The structural parameters are compared to those of related compounds in Table VIII. In contrast to bromodiborane,[6] which has a structure essentially identical with that of diborane except that a bromine atom replaces one of the nonbridging hydrogen atoms, ADB has substantially different structural parameters from those of diborane. It is of particular interest to note that the BH_2 groups are tilted from the plane perpendicular to the symmetry axis by 16.8 ± 0.1°.

ADB decomposes slowly at ambient temperature and DMADB is stable well above room temperature. The nitrogen atom in DMADB is so close to the center of mass that a ^{15}N substitution has more effect on the zero-point vibrations than on the moments of inertia. Hence the nitrogen coordinates in DMADB are not obtained by the Kraitchman substitution method. Furthermore the bridge hydrogen coordinates were not determined by a single substitution. A critical comparison for all structural parameters of ADB and DMADB is therefore not warranted. However there is little doubt that the small $+I$ effect of the two methyl groups in DMADB has minimal effect on its chemical bonding, which is dominated by the lone pair of electrons of the nitrogen atom. In fact the skeletal structural parameters in ADB and DMADB are virtually the same within experimental errors.

Acknowledgment. We gratefully acknowledge the support of the United States Air Force Office of Scientific Research under Grant 849-67 to the University of Southern California. Computer time was kindly provided by the University Computer Center.

Registry No. $^{14}NH_2{}^{11}B^{11}BH_5$, 52540-45-1; $^{14}NH_2{}^{10}B^{11}BH_5$, 52540-46-2; $^{14}NH_2{}^{10}B^{10}BH_5$, 52540-47-3; $^{15}NH_2{}^{11}B^{11}BH_5$, 52540-48-4; $^{15}NH_2{}^{10}B^{11}BH_5$, 52540-49-5; $^{14}NH_2{}^{11}B^{11}BD_tH_4$, 52540-50-8; $^{14}NH_2{}^{11}B^{10}BD_tH_4$, 52540-51-9; $^{14}NH_2{}^{10}B^{11}BD_tH_4$, 52540-52-0; $^{14}NH_2{}^{11}B^{11}BD_bH_4$, 52540-53-1; $^{14}NH_2{}^{11}B^{10}BD_bH_4$, 52540-54-2.

(6) A. C. Ferguson and C. D. Cornwell, *J. Chem. Phys.*, 53, 1851 (1970).